Medical Research Archives

European Society of Medicine

OPEN ACCESS

Published: November 30, 2023

Citation Kawaguchi AT., et al., 2023. Carboxyhemoglobin Particle Infusion, but not Carbon Monoxide Inhalation ameliorates Myocardial Infarction via Attenuated Oxidative Stress and In Situ Inflammation in a Rat Model. Medical Research Archives, [online] 11(11). https://doi.org/10.18103/mra.v11i11.4810

DOI:
https://doi.org/10.18103/mra.v11i11.4810

ISSN: 2375-1924

RESEARCH ARTICLE

Carboxyhemoglobin Particle Infusion, but not Carbon Monoxide Inhalation ameliorates Myocardial Infarction via Attenuated Oxidative Stress and *In Situ* Inflammation in a Rat Model

Akira T. Kawaguchi, MD, PhD[1,4]*, Tatsuhide Tanaka, PhD[2], Mariko Yamano, PhD[2], Hideaki Sumiyoshi, PhD[1], Hiroaki Kitagishi, PhD[3], Yoshiyuki Yamada, MD, PhD[4], Gen T. Kawaguchi, MD[5], Jacob Bergsland, MD[6]

[1]Department of Innovative Medical Science, Tokai University
[2]Department of Anatomy and Neuroscience, Nara Medical University
[3]Department of Molecular Chemistry and Biochemistry, Doshisha University
[4]Department of Pediatrics, Tokai University
[5]Department of Plastic Surgery, Tokai University
[6]Oslo University Hospital

*kawaguchi101060@gmail.com

ABSTRACT

Objective: Effects of PEGylated-carboxyhemoglobin bovine (SG) infusion and carbon monoxide (CO) inhalation were compared in a rat model of myocardial infarction (MI).

Methods: Lewis rats with induced MI received either 10 mL/kg of SG or of saline (SL), or 400 ppm CO inhalation (CO) daily for 3 days, 4 doses in total. On the fourth day, all animals had left ventricular (LV) functions studied by pressure-volume relationship analyses or *in-situ* myocardial gene expression by polymerase-chain reaction (PCR).

Results: Both SG infusion and CO inhalation increased the arterial carboxyhemoglobin fraction to 10%, which decreased the total O_2 content by 10% for 3 hours before returning to control level, except for the plasma hemoglobin (Hb) over 200 mg/dL 24 hours later, in SG rats. Four days after MI, the SL and CO rats had enhanced cardiac contraction and relaxation, while the SG rats had LV end-systolic pressure, and the isovolumic contraction as well as relaxation remained suppressed at the post-MI levels. PCR showed significant reductions in *in-situ* antioxidant transcriptional master regulator (Nrf2), its down-stream antioxidant response genes (Nqo-1), hypoxic signal transduction in SG compared to SL or CO rats with enhanced pro-inflammatory, pro-apoptotic genes, and myocardial damage. These cardiac indices were reversed 4 weeks after MI, when SG had less LV dilatation, dysfunction, and myoglobin loss than those with SL or CO.

Conclusion: The results suggest that repeated SG infusion, but not CO inhalation, generates less oxidative stress, reduces hypoxic responses, supports early hemodynamics, and alleviates cardiac compensation early after MI, resulting in attenuated LV dilatation, dysfunction, and myoglobin loss late after MI in this rat model.

Keywords: Artificial Oxygen Carrier, Myocardial Infarction, HBOCs, Carbon Monoxide, Oxidative Stress, Antioxidant Response genes, Cardiac Function

INTRODUCTION

Hemoglobin-based O_2 carriers (HBOCs)[1-5] are considered to carry O_2 as well as carbon monoxide (CO). Whereas exogenous CO has been reported to be vasodilatory, anti-inflammatory and cytoprotective in various end-organs[6-8], such as the brain[9], kidney[10], lung[11-13], and vasculature[14-16], parallel reduction in O_2-carrying capacity could be detrimental to cardiomyocytes and to the heart[17-20], which maintains homeostasis through idioventricular response[21] and neurohumoral regulation[22-27]. While infusion of an HBOC, PEGylated carboxyhemoglobin (COHb) bovine (SG)[2,28], early after myocardial infarction (MI) attenuated left ventricular (LV) dilatation, dysfunction, and fibrosis late after MI[29-30], the mechanisms of action are not clear - whether they are attributable to CO derived from SG or to the hemoglobin (Hb) particles *per se*. Since most of the myocardial damage had occurred within the first week of MI[29-30], changes occurring early after MI were studied in order to explore the mechanism(s) of action in the same rat model of SG infusion[30], which are compared with CO inhalation in terms of *in-situ* myocardial gene expression detected by real-time polymerase-chain reaction (PCR), LV functions analyzed by pressure-volume relationship (PVR)[31], LV size and contraction followed by echocardiography, and myocardial changes studied by histology and immunohistochemical (IHC) studies.

MATERIALS and METHODS

All experiments were approved by the Institutional Review Board of Tokai University. The animals received humane care as required by the institutional guidelines for animal care and treatment in experimental investigations according to the *Guide for the Care and Use of Laboratory Animals* (Institute of Laboratory Animal Resources, 1996).

Animals

Lewis rats (n=56) were purchased from Charles River Co. Ltd., (Yokohama, Japan) at 5 weeks of age. They were acclimated for 1 week before undergoing experiments in an animal cage under air conditioning at 26 ± 0.5°C with water and food *ad libitum*.

Protocol

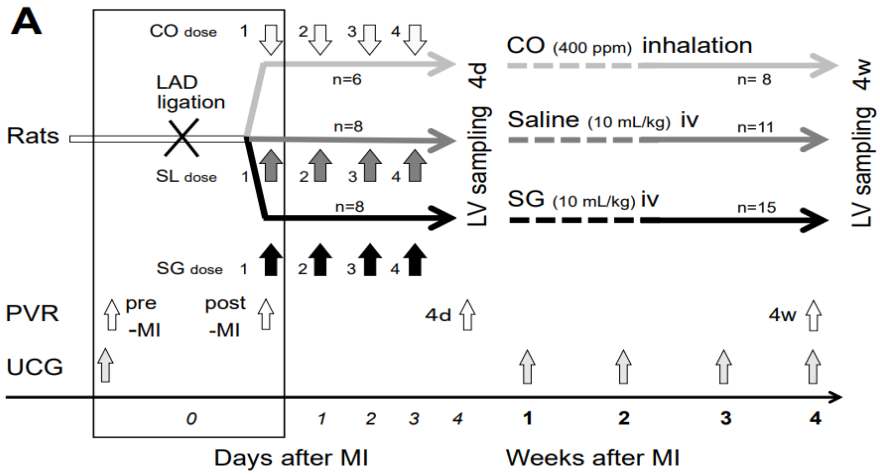

Figure 1A. Protocol. All rats underwent LAD ligation and received one of the three treatments: SG (10 mL/kg), saline, or 400 ppm CO inhalation, on Day 0 and daily thereafter for 3 days. They under-went echocardiography (UCG) and PVR studies before and at 4 days after MI, when LV was removed and sampled (4d). In the other sets of animals with MI, the same treatment was followed by weekly UCG, PVR studies, and sacrifice 4 weeks later (4w). The number of rats (n=) is listed along each process.

Rats were anesthetized with sevoflurane at 3%, orally intubated, and ventilated at 15 mL/kg of tidal volume with ambient air at 60 bpm with no end-expiratory pressure. An indwelling catheter was placed in the tail vein and saline was administered at 3 mL/hr. A rectal probe was placed to monitor body temperature, which was maintained at 36.5 ± 0.5°C with a water blanket, MEDI-Therm II (Gaymer Industries Inc, Orchard Park, NY, USA). The chest was entered via the 4th intercostal space, sevoflurane was reduced to 2%, and a tourniquet was placed around the descending aorta. Blood samples were drawn through the LV apex before and after PVR for calibration using a conductance catheter, and blood gas was analyzed using ABL800 Flex (Radiometer Medical ApS, Denmark). A catheter-tip manometer (Millar Instruments, Houston, TX, USA) and a conductance catheter (Unique Medical Co. Ltd, Tokyo, Japan) were placed through the LV apex to record LV PVR[30-31]. Afterload was changed by constricting the aortic tourniquet to develop both end-systolic and end-diastolic PVR. Acute volume-load was applied by acute intravenous infusion of saline (10 mL/kg at a rate of 0.1 mL/sec) to determine LV diastolic compliance. After recording control PVR (Pre-MI), the left anterior descending artery (LAD) was ligated and PVR was monitored for 10 min and recorded (Post-MI). Either SG (SG) or saline (SL) infusion, or CO (400 PPM) inhalation was started. After one of these treatments, blood samples were drawn, LV catheters were removed, and the chest was closed in three layers. Then, anesthesia was terminated, and the animal was extubated and returned to the cage (Fig. 1A).

PEGylated Carboxyhemoglobin Bovine (SANGUINATE)

SG was supplied by Prolong Pharmaceuticals, LLC (South Plainfield, NJ, USA). Its characteristics and pharmacokinetics were reported elsewhere[2,28-30]. Briefly, SG is bovine hemoglobin (Hb) bound to CO and modified with polyethylene glycol (PEG), resulting in an adduct with higher O_2-affinity ($P_{50}O_2$=12 mmHg, Fig.1B) compared to that of red blood cells (RBCs). The solution contains 3.7 ± 0.1 g/dL of bovine Hb with a high fraction of COHb (90.3 ± 3.6%) and a low rate of metHb (2.6 ± 0.7%). Because of the large amount

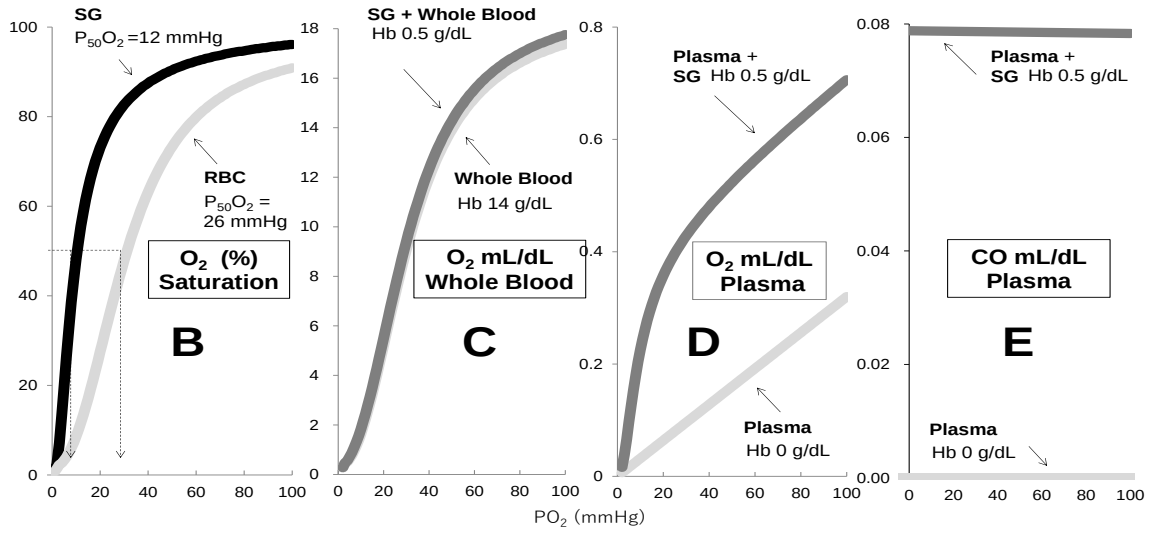

Figure 1.

B. SG ($P_{50}O_2$=12 mm Hg) may increase O_2 delivery to hypoxic tissue compared to RBC ($P_{50}O_2$=26 mm Hg).

C. SG 10 mL/kg infusion increased Hb by about 0.5 g/dL, and in whole blood to 14.5 g/dL.

D. The plasma O_2 content increased because of SG, where dissolved O_2 linearly increases with PO_2.

E. The plasma CO content decreases slowly with increasing pO_2 and dissolves a little to plasma.

COHb is set at 3% for a simulation. Modified from Ref 30.

of Hb in RBCs, 10 mL/kg of SG administration constitutes only 3.5% of Hb of the total in whole blood (Fig. 1C), as it represents most of the plasma Hb because there is little natural Hb in plasma (< 40 mg/dL, Fig. 1D). Once SG is intravenously infused, it releases CO and starts binding and releasing O_2 and CO depending on the surrounding O_2 and CO levels[30]. Naturally, CO is poorly dissolved in plasma and is tightly bound to Hb in the form of COHb. SG is removed from the circulation and is metabolized by the reticuloendothelial system, similar to RBCs, with an intravascular half-life of 12 hours in rats[2,28-30]. The amount of SG in whole blood was approximated as the plasma Hb, determined after centrifugation at 7000 G for 5 min.

Treatments and Follow-Ups

The first dose, 10 min after MI, either of SG or saline (10 mL/kg) was infused via a catheter in the tail vein at a rate of 0.5 mL/min in the same manner as in our study[30]. CO (400 ppm) was inhaled for 5 min by the same schedule (Fig. 1A). The treatment was repeated daily for 3 days at roughly 24-hour intervals, 4 doses in total. Repeated PVR and LV sampling (Fig. 1A) were carried out in different sets of animals 4 days (4d) and 4 weeks (4w) after MI when rats were anesthetized, intubated, and the chest was opened via the initial incision either to record repeated PVR, or for myocardial sampling.

LV sampling, RNA extract, and Real-time PCR

The heart was perfused with 100 mL of saline via the apex, and the LV was excised for PCR to the infarcted area (infarct), surrounding area (penumbra) and intact myocardium of the posterior wall between the pupillary muscles. The samples were minced in RNA-stabilizing solution (RNAlater, Thermo Fisher, Vilnius, Lithuania) and frozen at -80°C until real-time PCR analysis. Total RNA was extracted from cardiac muscular tissue using the NucleoSpin RNA kit (Macherey-Nagel, Düren, Germany) according to the manufacturer's instructions. Total RNA extracts were reverse transcribed using random primers and a QuantiTect Reverse Transcription kit (QIAGEN, Valencia, CA, USA) according to the manufacturer's instructions. Real-time PCR was performed using a LightCycler Quick System 350S (Roche Diagnostics, Indianapolis, IN, USA) with THUNDERBIRD SYBR qPCR Mix (Toyobo, Osaka, Japan). Hemoxigenase-1 (HO-1), hypoxia inducible factor 1-α (HIF-1α), NAD(P)H Quinone Dehydrogenase-1 (Nqo-1) and transcription factor NF-E2-related factor 2 (Nrf2) were determined as antioxidant genes. As inflammatory response, chemokines or cytokines such as CXC or CCL2 were determined. As apoptosis-related factors, Bcl-2-associated X protein (Bax), Caspase 3 (CAP3) and nitric oxide synthase (NOS) were determined. As the index of myocardial damage, heat-shock protein 90 (Hsp90AA1), nuclear factor kb1 (NFKb1) and BNP were ascertained. Complement and platelet activity were monitored in C3a receptor 1 (C3aR1). PCR sense and anti-sense primers are listed in Supplement 2.

Echocardiography

Under sevoflurane (2.5%) anesthesia, echocardiography (Aloka Co. Ltd., Tokyo, Japan) using a 3.5 MHz probe determined the LV end-diastolic dimension (LVDD) and end-systolic dimension (LVSD), and fractional shortening (%FS) was defined as (LVDD-LVSD)/ LVDD x 100. These measurements were repeated prior to the study (Pre) and weekly thereafter for four weeks after MI (4w).

Morphological Studies

The LV was excised and sliced at 2 mm thickness using a brain slicer, immersed in 4% paraformaldehyde and preserved overnight, then sliced into cross-sectional planes. These slices were stained with hematoxylin and eosin (H&E), and IHC analyses were performed using antibodies (Supplement 3) to detect the presence of myoglobin, macrophages with Iba1, bovine Hb, HO-1, HIF-1α, tumor necrosis factor α (TNFα), vascular endothelial growth factor (VEGF) and platelet-derived growth factor receptor β (PDGFRβ). In six additional rats, the whole heart was submitted to morphological studies with double and triple IHC staining to detect cytoplasmic or extracellular deposition of cytokines. The loss of myoglobin was considered a sign of fibrosis and was calculated individually. These measurements were averaged for each group and compared between groups.

Statistics

All data are expressed as mean ± SE. Statistical analysis was performed with GraphPad Prism for Windows, version 6.0 (GraphPad Software, San Diego, CA, USA). Differences among treatment groups were examined by Student t-test, Kruskal-Wallis test and Mann-Whitney-U test. A p value < 0.05 was considered statistically significant.

RESULTS

Effects on blood after SG infusion or CO inhalation

Intravenous SG (10 mL/kg) infusion and CO (400 ppm) inhalation for 5 min increased the arterial COHb fraction to 9.7 ± 0.2% (SG) and 10.0 ± 0.7% (CO), respectively, and then rapidly decreased to 5.6 ± 0.1% at 3 hours when the fraction was no longer statistically higher than that of untreated rats (Fig 2A). Between the groups the changes were similar in the other arterial blood components, including the total content of O_2 (tcO_2), total Hb (tHb), and plasma lactate (Fig. 2A). The fractions of O_2Hb, metHb and reduced Hb underwent similar changes among the groups and returned to pre-infusion level 3 hours later, as did COHb. Plasma lactate levels and arterial blood pH remained steady and comparable between treatments with SG and CO (Fig. 2B). In contrast, plasma Hb elevated over 600 mg/dL, stayed at over 500 mg/dL for the first 3 hours, and remained over 200 mg/dL for the initial 24 hours (Fig. 2C), which was higher than the plasma Hb before medication (32 ± 4 mg/dL).

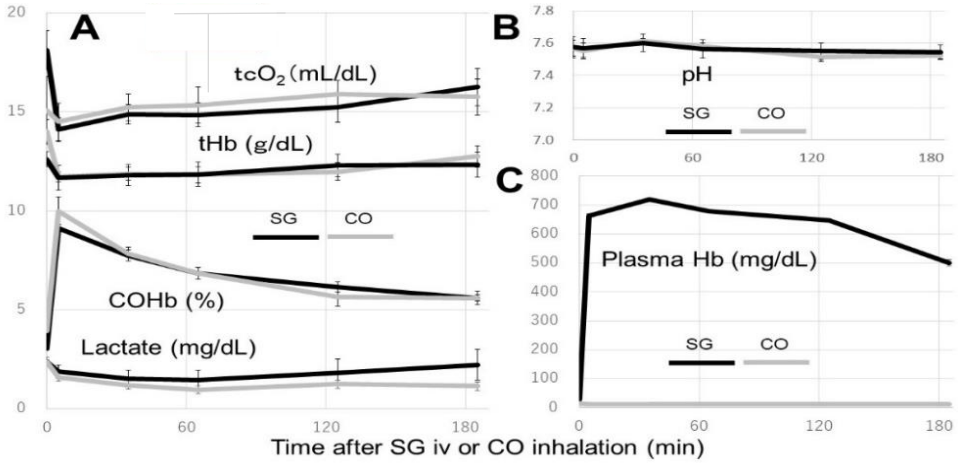

Figure 2. The infusion of SG (black lines) and CO inhalation (bright lines) changed total content of O_2 (tcO_2), total Hb (tHb), COHb (%), and plasma lactate similarly, and returned to baseline in 3 hours (**A**). There was no difference in plasma pH (**B**). In contrast, plasma Hb increased only after SG over 500 mg/dL for 3 hours and over 150 mg/dL for 24 hours (**C**).

Myocardial *In-Situ* Real-Time PCR Analyses

The mRNA expression levels of IL-1b, IL-6 and IL-10 were significantly suppressed both in the damaged area (infarct+penumbra) and in the intact myocardium in CO rats than in SG or SL (Fig. 3A). In contrast, differences in HO-1, HO-2, NOS2 or NOS3 were not significant in the damaged or intact myocardium among the treatment groups (Fig. 3B).

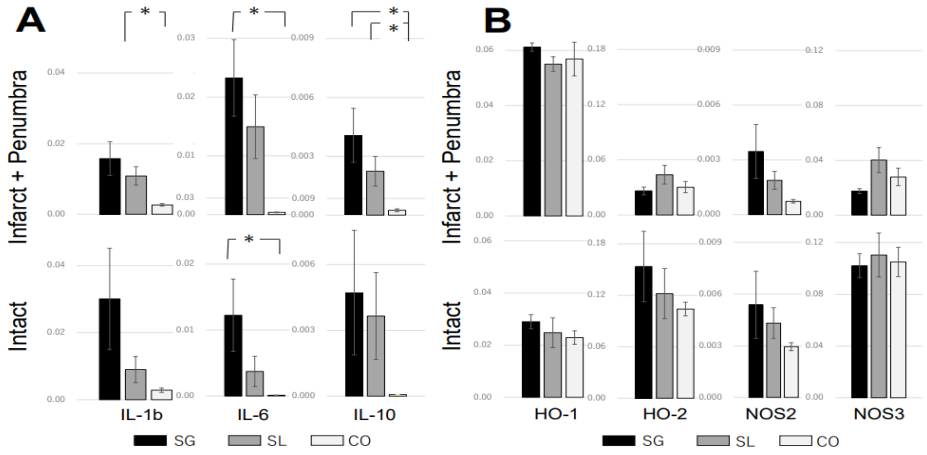

Figure 3. A. The mRNA levels of IL-1b, IL-6 and IL-10 in CO were significantly reduced in the damaged (upper panel) and in the intact myocardium (lower panel) compared to SG or SL. **B.** In contrast, differences in HO-1, HO-2, NOS2, or NOS3 were not significant in the damaged (upper panel) or intact myocardium (lower panel) among the groups. Asterisks depict $p < 0.05$

Differences in gene expression were observed mainly in the damaged area (Fig. 3C). The mRNA expression levels of antioxidant transcriptional master regulator Nrf2 and antioxidant gene Nqo-1 were significantly suppressed in SG (black bars) in the damaged area, where SL (gray bars) and CO (bright bars) rats showed similar trends against SG in HIF-1a, Cxcr3, Caspase 3, and BNP (Fig. 3C). The intact myocardium between papillary muscles showed no significant difference in the other genes tested among the treatment groups (not shown as Figures), making the damage / intact ratio (Fig. 3D) suppressed in CCL2, Hsp90AA1, TNF, NFKb1, and C3aR1, resulting in significant reduction in BAX and BNP expression in SG.

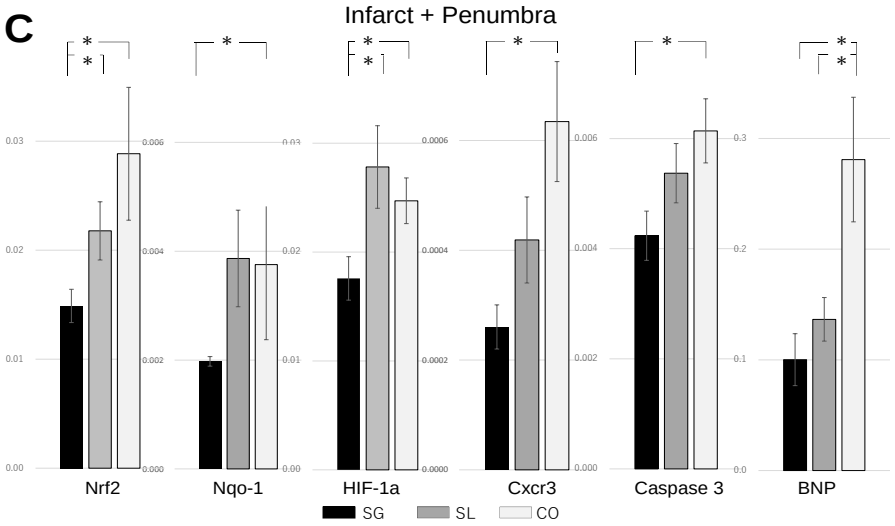

Figure 3C. In the damaged area, infarct and penumbra, (C), SG (black bars) had reduced expression than in SL (gray bars) or CO (bright bars). In contrast, CO showed a similar trend with SL except for BNP. Asterisks depict $p<0.05$.

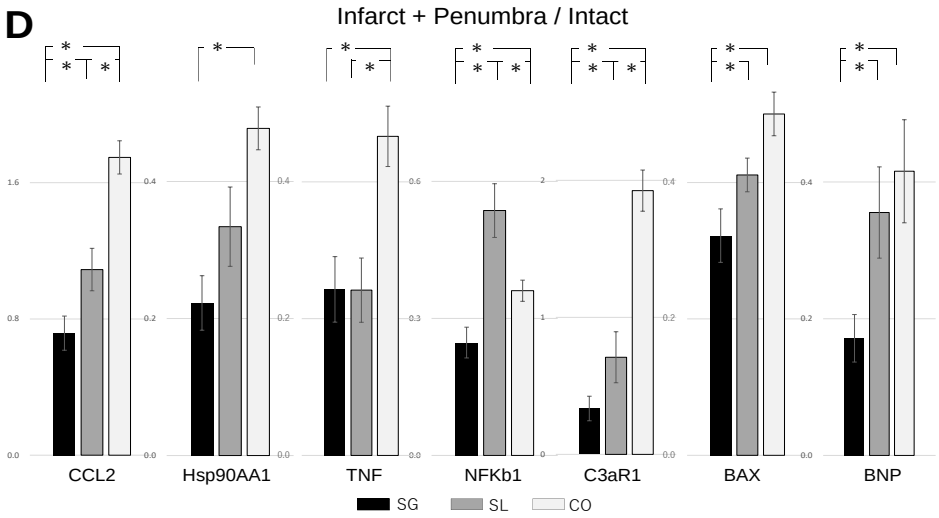

Figure 3D. The expression ratio of the damaged area (infarct + penumbra) / intact myocardium showed significant reduction in SG compared with SL or CO. In contrast, CO showed an enhanced expression similar to those of SL in most of tested genes. Legend is the same as for Figure 3C. Asterisks depict $p<0.05$

Pressure-Volume Relationship Analyses

There was no significant difference in cardiac indices immediately before and after induced MI, such as stroke volume (SV), heart rate (HR), cardiac output (CO), ejection fraction (EF), stroke work (SW), or pressure-volume area (PVA), suggesting that these indices were suppressed down to a comparable severity before treatments (Fig. 4A, 0d). Four days after MI and treatments (4d), indices such as ESPVR, ESP, max-positive dP/dt (Max+dP/dt) as well as max-negative dP/dt (Max-dP/dt) remained suppressed in SG rat compared to SL or CO (*), with indices enhanced to the pre-MI level (#). These functional indices, however, were mostly reversed 4 weeks after MI (4w), when SV, SW, max+dP/dt and max-dP/dt were significantly better preserved and recovered to the pre-MI levels in SG with the same EDPVR and EDP compared to the other treatment groups (*), which failed to regain pre-MI levels (#) 4w after MI (Fig. 4B).

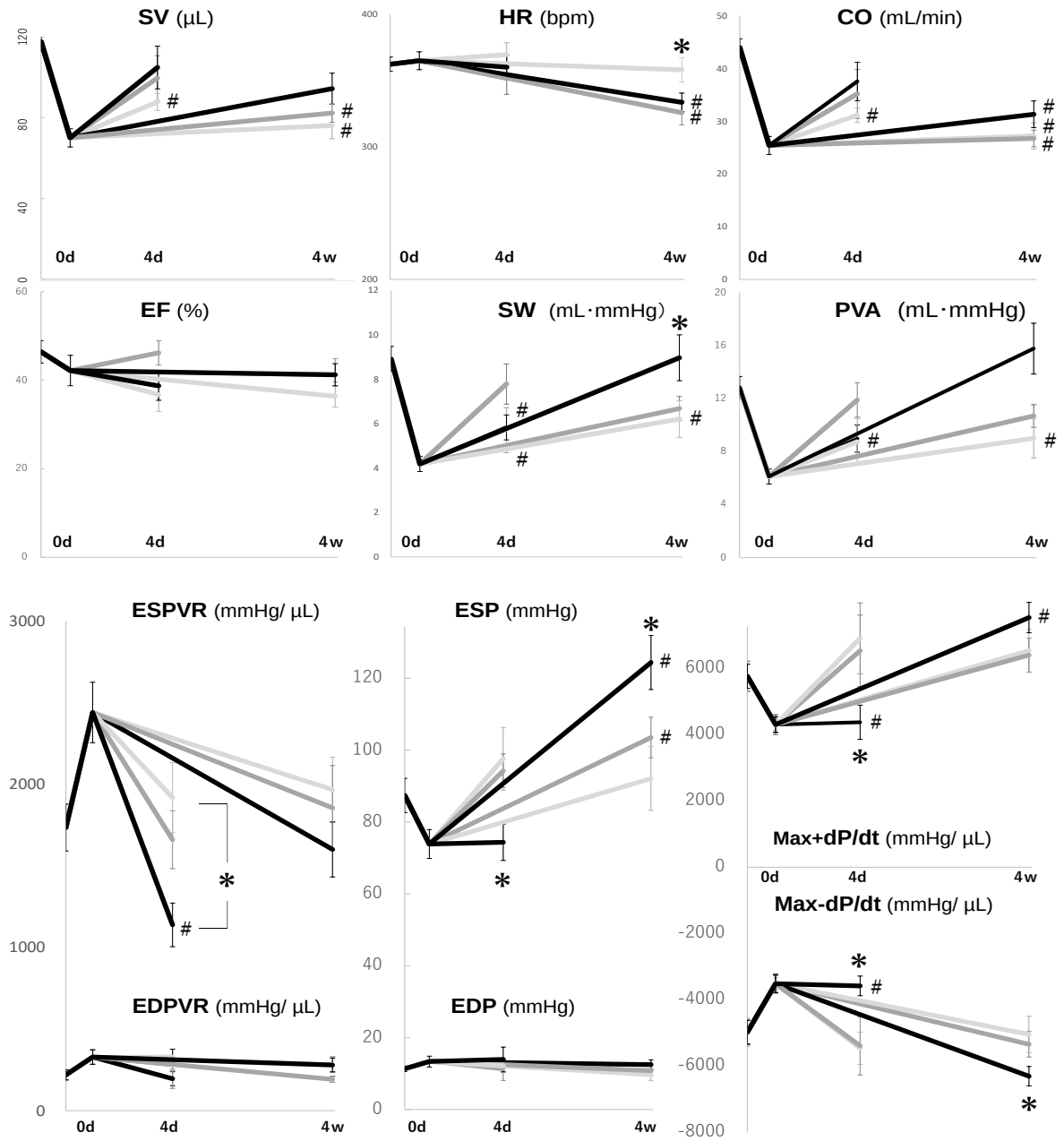

Figure 4. There was no significant difference in hemodynamic indices immediately before and after induced MI before treatments among groups on Day 0 (0d) and on Day 4 (4d). While ESPVR, ESP, max+dP/dt, and max-dP/dt were significantly suppressed 4 days after MI in SG rats (4d), these variables were mostly reversed and better preserved in SG rats 4w after MI (4w). **SG:** black lines, **SL:** gray lines, **CO:** bright lines. Asterisks (*) indicate $p < 0.05$ in the particular group against the other groups. Hash tags (#) depict $p < 0.05$ against pre-MI value.

Echocardiographic Follow-Up

Echocardiography recorded before (Pre) and 1 week after MI (1w) showed significant increase in LV dimensions, resulting in severe reduction in LV contraction as measured in FS and EF with no significant difference among the treatment groups against no MI control (#, Fig. 5). While LV dimensions remained rather stable thereafter in SG rats, LVSD kept increasing in SL and CO rats, rendering further LV dilatation and dysfunction in FS and EF at 2 weeks and thereafter against SG rats (*).

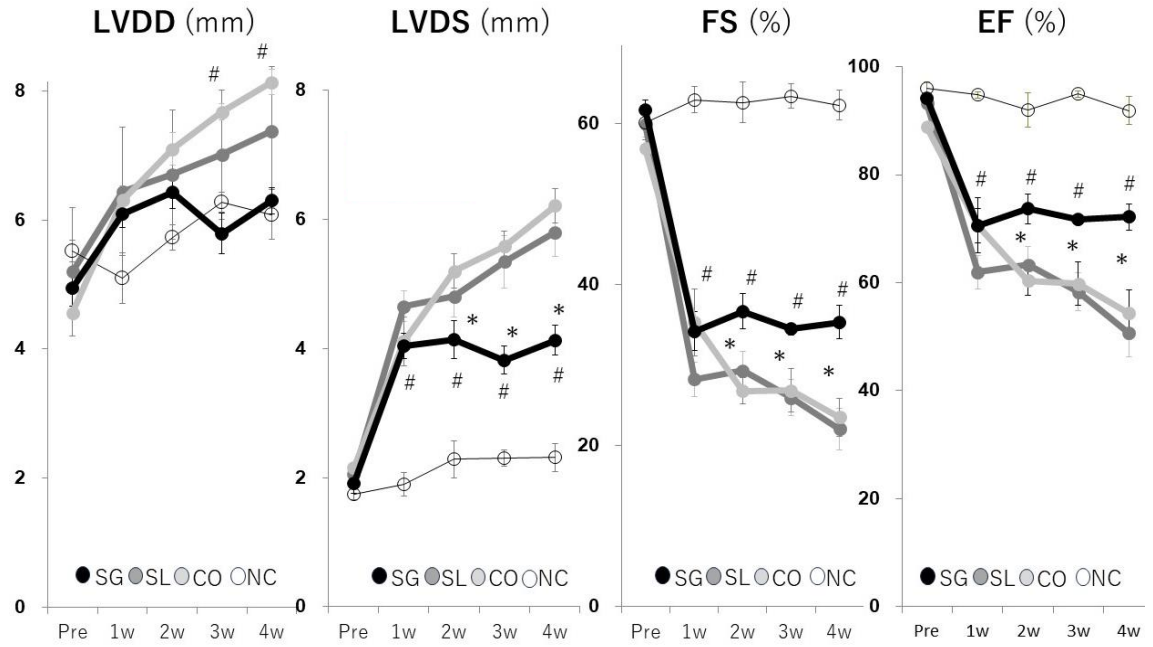

Fig.5. UCG follow-up showed no difference until 1 week after MI. Thereafter, SG rat kept LV size compared to SL or CO, where LVDD and LVSD kept increasing, to make a significant difference in FS 2 weeks and later. * p<0.05 against SG. # p<0.05 against no MI control (NC)

Pathohistological and IHC Studies

The representative macroscopic LV cross-section (left panels) 4 days after MI demarcated the area of infarction (Fig. 6A), which was stained with H&E (middle panels) and Iba1 (right panels) for the presence of macrophages in the same slice for SL (upper panels) and SG rat (lower panels). In the infarcted area and penumbra, there were losses of myoglobin and patchy infiltrating cells, which were largely Iba1-positive macrophages (Fig. 6B) (Supplemental Fig. B). In the other set of animals 4 weeks after MI (Fig. 6C), the fraction of loss of myoglobin was significantly suppressed in rats treated with SG (black bar) as compared to the rats treated with saline (SL, gray bar) or CO inhalation (CO, bright bar) (Supplemental Fig. A).

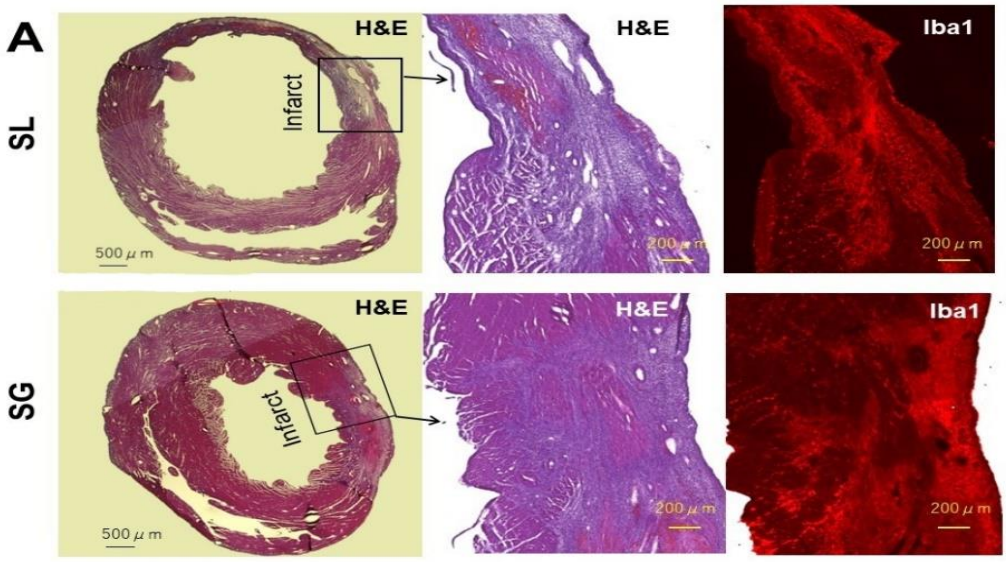

Figure 6.The representative macroscopic LV cross-section (left panels) 4 days after MI demarcated the area of infarction, which was stained with H&E (middle panels) and Iba1 (right panels) for the presence of macrophages in the same slice for SL (upper panels) and SG rats (lower panels).

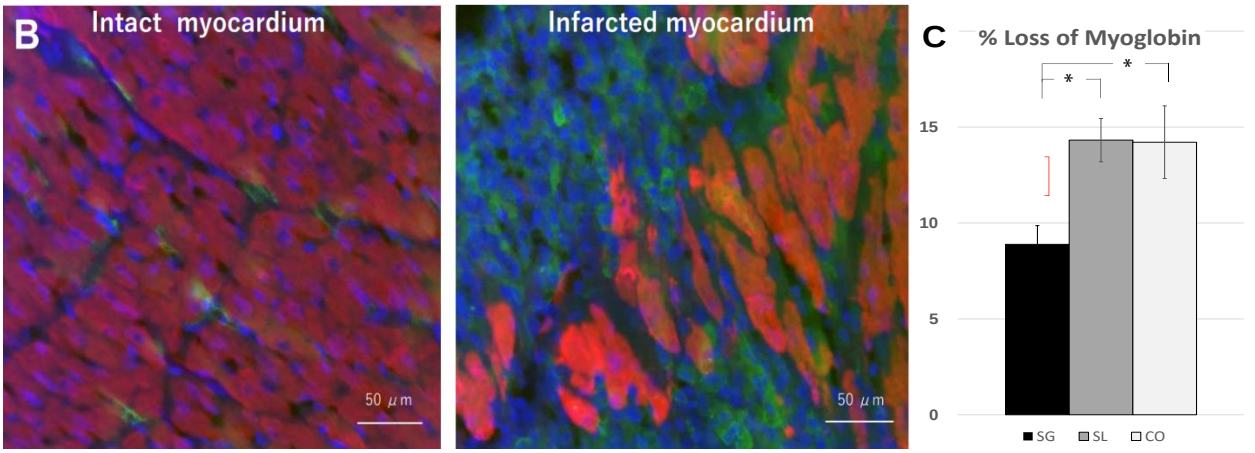

Fig. 6. B. IHC staining for myoglobin (red), Iba1 (green), and DAPI (blue) showed the intact myocardium (left) with little cellular infiltration and infarct (right) with reduced myocardium and infiltrating Iba1-positive macrophages. **C (Supplemental Fig. B).** The fraction of loss of myoglobin (Supplemental Fig. A) 4 weeks after MI was significantly suppressed in rats treated with SG (black bar) compared to the rats treated with SL (gray bar) or CO inhalation (bright bar). Asterisks (*) depict $p < 0.05$.

DISCUSSION

Exogenous CO application and Endogenous CO Behavior

Based on studies of exogenous CO distribution and excretion[32-33], inhaled CO linearly increased intravascular COHb[32-34] and decreased after cessation of inhalation as a multi-compartment model. In the current study, COHb was arbitrarily set at 10% to compare with SG infusion[30]. In contrast, selective depletion of endogenous CO induced HO-1 to maintain the CO level constant as intravascular ferrous/ferric homeostasis[35]. While 10% of COHb may seem to be low like after smoking a cigarette[36], the *in-situ* expression of IL-1b, IL-6, and IL-10 in CO rats was significantly suppressed in the infarcted as well as intact myocardium (Fig. 3A), as was reported in the airway[11-13,37]. Nonetheless, the COHb level was much lower than that employed in other systemic applications, 18%, and 26% to 39%[3], where the addition of CO to Hb vesicle[3] or RBC[3,38] was reported to be lifesaving after induced hemorrhage and transfusion. Typical of such condition were hemorrhage and transfusion, regarding which Natanson at al[5] reported increased incidence of MI and death over controls in clinical trials testing five different cell-free HBOCs. The addition of CO to MP4, one of the five, reduced the MI size in rats with a COHb fraction of 7.6% or lower[4]. As such, in addition to CO or antioxidant property, it is important to possess O_2 carrying capability[39] to treat blood loss, and hemolytic as well as anemic conditions such as hemorrhage[3,4,38], cerebral malaria[40] and sickle cell disease[41]. While the effect of COHb over 30% was experimentally studied[42], such increase in COHb would not ameliorate, but rather jeopardize the myocardium, primarily by a reduction of O_2 delivery to the myocardium as an end-organ[33], and secondarily by an autonomic response to compensate for reduced O_2 delivery[22-23,43], resulting in hemodynamic instability and finally premature cardiac death from CO intoxication[34,44]. Although SG and CO treatment induced a comparable COHb level that releases CO to stabilize intravascular free-heme[35], the differences result from the presence of plasma Hb particles, SG[28-30] or HBOCs[45-46], delivering O_2 or CO to ameliorate

hypoxic responses[47] regardless of peripheral perfusion status, such as in a pathologic condition[48], ischemia and/or re-perfusion[18,28-29] or infarction[30,49]. Such difference may be acquired from improved microcirculation by HBOCs[4,47-50] rather than from RBC after CO inhalation.

In-situ Myocardial Gene Expression

The reason for the effects of CO inhalation limited only on IL-1b, IL-6 and IL-10 (Fig. 3A) is not clear, but they might have been derived from the direct and local exposure to the airways[11-13,37] like those from CO-releasing molecules[6,8]. The absence of differences in HO-1, HO-2, NOS2 and NOS3[51-52] may suggest that there is little difference in Hb catabolism[53] or NO metabolism[54] among the groups (Fig. 3B). Instead, Nrf2, Nqo-1 and HIF-1α were significantly suppressed only in SG rat, suggesting that the myocardial protection by SG might not pass along the CO/HO axis[13,55] but rather via the reduced oxidative stress[56-59] and attenuated hypoxic responses[47] with aerobic energy metabolism, which were reported to be providing cardiac energetics[20] and fatigue resistance in the skeletal muscle[18]. Thus, the expression of HIF-1α gene in the infarct (Fig. 3C) was reduced in SG, suggesting that hypoxic signal transduction was attenuated as reported in various tissue/organs under hypoxia treated with LEH[47,60-61]. As a result, cytokines[62] in response to MI, such as CCL[37,63-64] and CXCR3[65-66], were significantly attenuated in SG compared to in SL or CO. These pro-inflammatory genes were transduced to regulators, such as HSP90aa1[67-68], TNFα[69], NFkb[46,70-71], and pro-apoptotic genes[72], including BAX[73] and CASP3[74]. In addition, complement activation[75] was significantly suppressed only in the damaged myocardium of SG rats (Fig. 3C). As described above, the significant changes in *in-situ* gene expression after SG treatment were mostly anti-oxidative[69], anti-inflammatory[46,62], and anti-apoptotic[69], with reduced BNP (4d) resulting in improved heart repair late after MI (4w)[69].

Myocardial Function and LV Dimensions

There was no significant difference in hemodynamic variables immediately before and after the induction of MI (Fig. 4A), suggesting that MI was induced at a similar severity among the treatment groups. After repeated treatments (4d), hemodynamic variables such as SV, HR, and CO were comparable among the treatment groups[24-26], while LV indices of contraction (max+eP/dt) and relaxation (max-dP/dt) were enhanced to pre-MI level, reflecting the idioventricular and neurohumoral activation of myocardium in SL and CO rats[21,24]. Such exaggeration early after MI (4d) was considered as a compensatory mechanism[21-23] for reduced cardiac output at the cost of myocardial hyperactivation, which would result in more damage as simultaneously observed in the enhanced pro-inflammatory and pro-apoptotic genes with elevated BNP production (Fig. 3b). In contrast, the SG rat had max+dP/dt and max-dP/dt, and ESP[21,24] remained suppressed as the immediate post-MI level[26-27] (#), which made a significant difference from SL or CO treatments (*). A similar relationship was observed early after myocardial ischemia treated with LEH[76], where SV and EF remained reduced compared to control rats. While such myocardial changes were not apparent in hemodynamics, LV size or function by UCG until 2 weeks after MI, the end-systolic rather than the end-diastolic

dimension became progressively increased thereafter in SL and CO, creating a significant difference against SG rat. As a result, the early differences (4d) were mostly reversed 4 weeks after MI, as in our previous observation late after MI[30].

Limitations

The current cross-sectional study was carried out to explore the mechanism(s) of action; real-time PCR detects mRNA signaling at the exact sampling time and location, which is considered to reflect the real-time hemodynamic needs that were realized by cardiac compensation via neurohumoral regulation[21-23]. Since the link is plausible but still speculative, further study is necessary to clarify the causative relationship. In this regard, Bax and Casp3 gene expressions may be timely and suitable for monitoring apoptotic activity at the same time (4d), since their frequency was reported to shift from the penumbra early after MI, to involve even the intact myocardium 4 weeks after MI[72]. The same was true in histological changes (Supplemental Fig. A-B), which lag the relationship between gene signaling and myocardial function. Although such cardiac compensation and evolution of apoptosis could conceal the hemodynamic difference early after MI, it became obvious in the LV dilatation and dysfunction by UCG and loss of myoglobin beyond the acute phase of MI as observed in the previous[30] and current studies.

CONCLUSION

The results collectively suggest that repeated SG infusion, but not CO inhalation, early after MI attenuated, rather than enhanced, cardiac contraction and relaxation, when PCR showed significant reduction in antioxidant transcriptional master regulator (Nrf2), its downstream antioxidant response genes (Nqo-1), pro-inflammatory factors, hypoxic signal mediators, complement activator and pro-apoptosis genes with less myocardial damage 4 days after MI. These changes were considered to originate from plasma Hb particles or HBOCs and result in preserved LV function and reduced loss of myoglobin 4 weeks after MI. Further studies are needed to explore the exact mechanism(s) and dose and timing of its administration for myocardial ischemia and/or infarction.

Conflict of Interest Statement:

None

Funding Statement:

This study was supported in part by

1. Scientific Support KAKENHI 15H2569, 21K07833, and 21K08651. JSPS, Japan
2. Project Kenkyu, Tokai University

Acknowledgement Statement:

The authors thank the Medical Science College Office, Tokai University, for technical assistance.

REFERENCES:

1. Kaneda S, Ishizuka T, Goto H, Kimura T, Inaba K, Kasukawa H. LEH, TRM645: current status of development and important issues for clinical application. *Artif Organs* 2009;33:146-52.

2. Abuchowski A. Sanguinate (PEGylated Carboxyhemoglobin Bovine): Mechanism of action and clinical update. *Artif Organs* 2017:41:346-350.

3. Sakai H, Horinouchi H, Tsuchida E, Kobayashi K. Hemoglobin vesicles and red blood cells as carriers of carbon monoxide prior to oxygen for resuscitation after hemorrhagic shock in a rat model. *Shock* 2009;31:507-14.

4. Vandegriff KD, Young MA, Lohman J, et al. CO-MP4, a polyethylene glycol-conjugated haemoglobin derivative and carbon monoxide carrier that reduces myocardial infarct size in rats. *Br J Pharmacol* 2008;154:1649-61.

5. Natanson C, Kern SJ, Lurie P, Banks SM, Wolfe SM. Cell-free hemoglobin-based blood substitutes and risk of myocardial infarction and death: a meta-analysis. *JAMA* 2008;299: 2304-12.

6. Foresti R, Bani-Hani MG, Motterlini R. Use of carbon monoxide as a therapeutic agent: promises and challenges. *Intensive Care Med.* 2008;34:649-58. Doi 10.1007/s00134-008-1011-1.

7. Bauer I, Pannan BHJ. Bench-to-bedside review: Carbon monoxide-from mitochondrial poisoning to therapeutic use. *Crit Care* 2009;13:220 Doi:10.1186/cc7887.

8. Motterlini R, Otterbein LE. The therapeutic potential of CO. *Nature Medicine* 2010;10: Doi:10.1038/nrd3228.

9. Zeynalov E, Dore S. Low dose of carbon monoxide protect against experimental focal brain ischemia *Neurotox Res* 2009;15;133-137. Doi:10.1007/s12640-009-9014-4.

10. Ruan Y, Wang L, Zhao, Yao Y, Chen S, Li J, et al. Carbon monoxide potently prevents ischemia-induced high-mobility group box 1 translocation and release and protects against lethal renal ischemia-reperfusion injury. *Kidney international.* 2014;86:525-37.

11. Kim SK, Joe Y, Chen Y, et al. Carbon monoxide decreases interleukin-1β levels in the lung through the induction of pyrin. *Cellular & Molecular Immunol.* 2017;14:349-59.

12. Ning W, Choi AMK, Li C. Carbon monoxide inhibits IL-17-induced IL-6 production through the MAPK pathway in human pulmonary epithelial cells. *Am J Physiol Lung Cell Mol Physiol.* 2005;289:L268-L273.

13. Zhang X, Ding M, Zhu P, Nalley CM, et al. New insights into the Nrf-2/HO-1 signaling axis and its application in pediatric respiratory diseases. *Oxidative Med Cellular Longevity* 2019; Article ID3214196. Doi org/10.1155/2019/3214196

14. Coceani F. Carbon monoxide in vasoregulation. The promise and the challenge. *Circ Res* 2000;86:1184-6.

15. Liu XM, Chapman GB, Peyton KJ, Schafer AI, Durante W. Carbon monoxide inhibits apoptosis in vascular smooth muscle cells. *Cardiovasc Res* 2002;55:396-405.

16. Motterlini R, Foresti R, Vandegriff K, Intaglietta M, Winslow RM. Oxidative-stress response in vascular endothelial cells exposed

to acellular hemoglobin solutions. *Am J Physiol* 1995;269: (Heart Circ Physiol 38):H648-H655.

17. Suliman HB, Carraway MS, Ali AS, Raynolds CM, Welty-Wolf KE, Piantadosi CA. The CO/HO system reverses inhibition of mitochondrial biogenesis and prevents murine doxorubicin cardiomyopathy. *J Clin Investig*. 2007;117:3730-41.

18. Kawaguchi AT, Tamaki T. Artificial Oxygen carrier improves fatigue resistance in slow muscle but not in fast muscle in a rat in situ model. *Artif Organs.* 2019.

19. Nakao A, Toyokawa H, Abe M, et al. Heart allograft protection with low-dose carbon monoxide inhalation: effects on inflammatory mediators and alloreactive T-cell responses. *Transplantation* 2006;81220-230.

20. Lavitrano M, Smolenski RT, Musumeci A, et al. Carbon monoxide improves cardiac energetics and safeguards the heart during reperfusion after cardiopulmonary bypass in pigs. *FASEB J* 2004 Doi: 10.1096/fj.03-0996fje.

21. Gilbert TC, Leite-Moreira AF, De Hert SG. Relaxation-systolic pressure relation. *Circulation* 1997;95:745-52.

22. Hartupee J and Mann DL. Neurohumoral activation in heart failure with reduced ejection fraction. *Nat Rev Cardiol* 2017; 14:30-38.

23. Parrish DC, Gritman K, Van Winkle DM, Woodward WR, Barder M, Habecker BA. Postinfarct sympathetic hyperactivity differentially stimulates expression of tyrosine hydroxylase and norepinephrine transporter. *Am J Physiol Heart Circ Physiol* 2008; 294: H99-H106.

24. Henning RJ, Levy MN. Effects of autonomic nerve stimulation, asynchrony, and load on dP/dtmax and dP/dtmin. *Am J Physiol* 1991;260 (Heart Circ Physiol 29):H1290-H1298.

25. Jardine DL, Charles CJ, Ashton RK, et al. Increased cardiac sympathetic nerve activity following acute myocardial infarction in a sheep model. *J Physiol* 2005;565:325-33.

26. Burwash IG, Morgan DE, Koilpillai CJ, Blackmore GL, Johnstone DE, Armour JA. Sympathetic stimulation alters left ventricular relaxation and chamber size. *Am J Physiol* 1993; 264(Regulatory Integrative Comp Physiol 33): R1-R7.

27. Zhang DY, Anderson AS. The sympathetic nervous system and heart failure. *Cardiol Clin* 2014;32:33-vii. Doi:10.1016/j.ccl.2013.09.010.

28. Klaus JA, Kibler KK, Abuchowski A, Koehler RC. Early treatment of transient focal cerebral ischemia with bovine PEGylated carboxy hemoglobin transfusion. *Artif Cell Blood Substit Biotechnol* 2010; 38:223-9.

29. Ananthakrishnan R, Li Q, Karen M, et al. Carbon monoxide form of PEGylated hemoglobin protects myocardium against ischemia/reperfusion injury in diabetic and normal mice. *Artif Cell Nanomed Biotechnol* 2013; Early Online: 1-9.

30. Kawaguchi AT, Salybekov AA, Yamano M, Kitagishi H, Sekine K, Tamaki T. PEGylated carboxyhemoglobin bovine (SANGUINATE) ameliorates myocardial infarction in a rat model. *Artif Organs* 2018;42:1174-84. doi: 10.1111/aor.13384

31. Sagawa K, Maugahan L, Suga H, Sunagawa K. Cardiac contraction and the pressure-volume relationship. Sagawa K, Maugahan L, Suga H, Sunagawa K, eds. 1988 by Oxford University Press, Inc. 200 Madison Avenue, NY, NY 10016

32. Luomanmaki K, Coburn RF. Effects of metabolism and distribution of carbon monoxide on blood and body stores. *Am J Physiol* 1969;217:354-363.

33. Mao Q, Kawaguchi AT, Mizobata S, Mottelini R, Foresti R, Kitagishi H. Sensitive quantification of carbon monoxide in vivo reveals a protective role of circulating hemoglobin in CO intoxication. *Communication Biology* 2021;4:425

34. Mao Q, Zhao X, Kiriyama A, et al. A synthetic porphyrin as an effective dual antidote against carbon monoxide and cyanide poisoning. *PNAS* 2023;120:e2209924120

35. Kitagishi H, Minegishi S, Yumura A, et al. Feedback response to selective depletion of endogenous carbon monoxide in the blood. *J Am Chem Soc* 2016;138:5417-25.

36. Cronenberger C, Mould DR, Roethig HJ, Sarkar M. Population pharmacokinetic analysis of carboxy-hemoglobin concentration in adult cigarette smokers. *Br J Clin Pharmacol* 2008;65:30-9.

37. Morse D, Pischke SE, Zhou Z, et al. Suppression on inflammatory cytokine production by carbon monoxide involves the JNK pathway and AP-1. *J Biol Chem* 2003;278:36993-8.

38. Cabrales P, Tsai AG, Integrietta M. Hemorrhagic shock resuscitation with carbon monoxide saturated blood. *Resuscitation* 2007;72:306-18.

39. Cooper CE, Silkstone GGA, Simons M, et al. Engineering hemoglobin to enable homogenous PEGylation without modifying protein functionality. *Biomater Sci* 2020;8:3896. Doi:10.1039/c9bm01773a

40. Pamplona A, Ferreira A, Balla J, et al. Heme oxygenase-1 and carbon monoxide suppresses the pathogenesis of experimental cerebral malaria. *Nature Med.* 2007;13:703-10.

41. Nalley CM, Abucowski A, Hsu S, Lanzkron S. Successful use of carboxyhemoglobin bovine as an emergency treatment for severe anemia in a patient with sickle cell disease and hyperhemolysis: A case report. *Blood* 2014;124:4928.

42. Fujimoto H, Ohno M, Ayabe S, et al. Carbon monoxide protects against cardiac ischemia-reperfusion injury in vivo via MAPK and Akt-eNOS pathways. *Arterioscler Thromb Vasc Biol* 2004;24:1848-53.

43. Chu LM, Shaefi S, Byrne JD, Alves de Souza RW, Otterbein LE. Carbon monoxide and a change of heart. *Redox Biol* 2021;48:102183 Doi.org/10.1016/j.redox.2021102182

44. Delvau N, PenalozaA, Franssen V, Thys F, Roy PM, Hanson P. Unexpected carboxy-hemoglobin half-life during cardiopulmonary resuscitation: a case report. *Intern J Emer Med* 2023;16:22

45. Zhang J, Cao S, Kwansa H, Crafa D, Kibler KK, Koehler RC. Transfusion of hemoglobin-based oxygen carriers in the carboxy state is beneficial during transient focal cerebral ischemia. *J Appl Physiol* 2012;113:1709-17.

46. Wang Q, Hu L, Hu Y, et al. Carbon monoxide-saturated hemoglobin-based

oxygen carriers attenuate high-altitude-induced cardiac injury by amelioration of the inflammation response and mitochondrial oxidative damage. *Cardiology* 2017;136:180-91.

47. Kawaguchi AT. Artificial oxygen carrier to regulate hypoxic signal transduction. *Artif Organs* 2014;38:617-20. Doi:10.1111/aor.12372

48. Fukui T, Kawaguchi AT, Takekoshi S, Miyasaka M, Sumiyoshi H, Tanaka R. Liposome-encapsulated hemoglobin accelerates skin wound healing in diabetic dB/dB mice. *Artif Organs*. 2017;41:319-326. Doi: 10.1111/aor.12864

49. Kawaguchi AT, Kurita D, Furuya H, Yamano M, Ogata Y, Haida M. Liposome-encapsulated hemoglobin alleviate brain edema after permanent occlusion of the middle cerebral artery. *Artif Organs* 209;33:153-8.

50. Fukuta T, Ishii T, Asai T, et al. Real-time trafficking of pegylated liposomes in the rodent focal brain ischemia analyzed by positron emission tomography. *Artif Organs.* 2014;38:662-6. Doi:10.1111/aor.12350.

51. Umar S, Laarse AVD. Nitric oxide and nitric oxide synthase isoforms in the normal, hypertrophic, and failing heart. *Mol Cell Biochem* 2010;333:191-201.

52. Janssen S, Pokreisz P, Schoonjans L, et al. Cardiomyocyte-specific overexpression of nitric oxide synthase 3 improves left ventricular performance and reduces compensatory hypertrophy after myocardial infarction. *Circ Res* 2004;94:1256-62.

53. Wu L, Wang R. Carbon monoxide: Endogenous production, physiological functions, and pharmacological applications. *Pharmacol Rev.* 2005;57:585-630.

54. Tsai AG, Cabrales P, Manjula BN, Acharya SA, Winslow RM, Intaglietta M. Dissociation of local nitric oxide concentration and vasoconstriction in the presence of cell-free hemoglobin oxygen carrier. *Blood.* 2006;108:3603-10.

55. Loboda A, Damulewicz M, Pyza E, Dulak J. Role of Nrf2/HO-1 system in development, oxidative stress response and disease: an evolutionarily conserved mechanism. *Cell Mol Life Sci* 2016;73:3221-47.

56. Kobayashi M, Yamamoto M. Molecular mechanisms activating the Nrf2-Keap1 pathway of antioxidant gene regulation. *Antioxid Redox Signal.* 2005;7:385-94.

57. Ndisang JF. Synergistic interaction between heme oxygenase (HO) and nuclear-factor E2-related factor-2 (Nrf2) against oxidative stress in cardiovascular related diseases. *Current Pharmaceu Design* 2017;23:1465-70 [Abs].

58. Shinjo T, Tanaka T, Okuda H, et al. Propofol induces nuclear localization of Nrf2 under conditions of oxidative stress in cardiac H9c2 cells. *PLoS ONE.* 2018 Doi: 10.1371/ journal.pone0196191 April 24, 2018

59. Huang Y, Li W, Su ZY, Kong AN. The complexity of the Nrf2 pathway: Beyond the antioxidant response. *J Nutr Biochem* 2015;26:1401-13.

60. Nogami Y, Kinoshita M, Takase B, et al. Liposome-encapsulated hemoglobin transfusion rescues rats undergoing progressive hemodilution from lethal organ hypoxia without scavenging nitric oxide. *Ann Surg* 2008;248:310-319.

61. Tekin D, Dursun AD, XI L. Hypoxia inducible factor 1 (HIF-1) and cardioprotection. *Acta Pharmacologica Sinica* 2010;31:1085-94

62. Frangogiannis NG, Smith CW, Entman ML. The inflammatory response in myocardial infarction. *Cardiovasc Res* 2002;53:31-47.

63. Dewald O, Zymeck P, Winkelmann K, et al. CCL2/monocyte chemoattractant protein-1 regulates inflammatory responses critical to healing myocardial infarcts. *Circ Res* 2005;96:881-9.

64. Zhang H, Yang K, Chen F, et al. Role of the CCL2-CCR2 axis in cardiovascular disease: pathogenesis and clinical implications. *Front Immunol* 13:975367

65. Szentes V, Gazdag M, Szokodi I, Dezsi CA. The role of CXCR3 and associated chemokines in the development of atherosclerosis and during myocardial infarction. *Front Immunol* 2018;9:1932. Doi: 10.3389/fimmu.2018.01930.

66. Bujak M, Dobaczewski M, Gonzalez-Quesada C, et al. Induction of the CXC chemokine interferon-γ-inducible protein 10 regulates the reparative response following myocardial infarction. *Circ Res* 2009;105:973-83.

67. Ranek MJ, Stachowski MJ, Kirk JA, Willis MS. The role of heat shock proteins and co-chaperons in heart failure. *Phil Trans R Soc B* 373:20160530
Doi:org/10.1098 /rstb.2016.0530

68. Shi Y, Baker JE, Zhang C, et al. Chronic hypoxia increases endothelial nitric oxide synthase generation of nitric oxide by increasing heat shock protein 90 association and serine phosphorylation. *Circ Res* 2002;91:300-309.

69. Prabhu SD, Frangoglannis NG. The biological basis for cardiac repair after myocardial infarction: from inflammation to fibrosis. *Circ Res* 2016;119:91-112.

70. Misra A, Haudek SB, KnuefermannP, et al. Nuclear factor-kB protects the adult cardiac myocyte against ischemia-induced apoptosis in a murine model of acute myocardial infarction. *Circulation* 2003;108:3075-8.

71. Fiordelisi A, Iaccarino G, Morisco C, Coscioni E, Sorriento D. NFKappaB is a key player in the crosstalk between inflammation and cardiovascular diseases. *Int J Mol Sci* 2019;20:1599. Doi:10.3390/ijms20071599

72. Palojoki E, Saraste A, Eriksson A, et al. Cardiomyocyte apoptosis and ventricular remodeling after myocardial infarction in rats. *Am J Physiol Heart Circ Physiol* 2001;280:H2726-H2781.

73. Korshunova AY, Blagonravov ML, Neborak EV, et al. BCL2-regulated apoptotic process in myocardial ischemia-reperfusion injury. *Int J Mol Medicine* 2021;47:23-36.

74. Abbate A, Biondi-Zoccai GGL, Baldi A. Pathophysiologic role of myocardial apoptosis in post-infarction left ventricular remodeling. *J Cell Physio* 2002;193:145-153

75. Tanhehco EJ, Yasojima K, McGeer PL. Preconditioning reduces myocardial complement gene expression in vivo. *Am J Physiol Heart Circ Physiol* 2000;279: H1157-H1165.

76. Wysoczynski M, Solanki M, Borkowska S, et al. Complement component 3 is necessary to preserve myocardium and myocardial function in chronic myocardial infarction. *Stem Cells* 2014;32:2502-15. Doi:10.1002/stem.1743.

77. Kawaguchi AT, Yamano M. LEH, artificial O_2 carrier, preserves VO_2 and protects myocardium after myocardial ischemia/ reperfusion in the rat. *Circulation.* 124 (suppl_21), A12215-A12215 [Abs]

78. Naito Y, Takagi T, Higashimura Y. Heme oxygenase-1 and anti-inflammatory M2 macrophages. *Archives Biochemistry and Biophysics*. 2014;564:83-8.

SUPPLEMENTAL FIGURES

Figure A. IHC Staining for Myoglobin

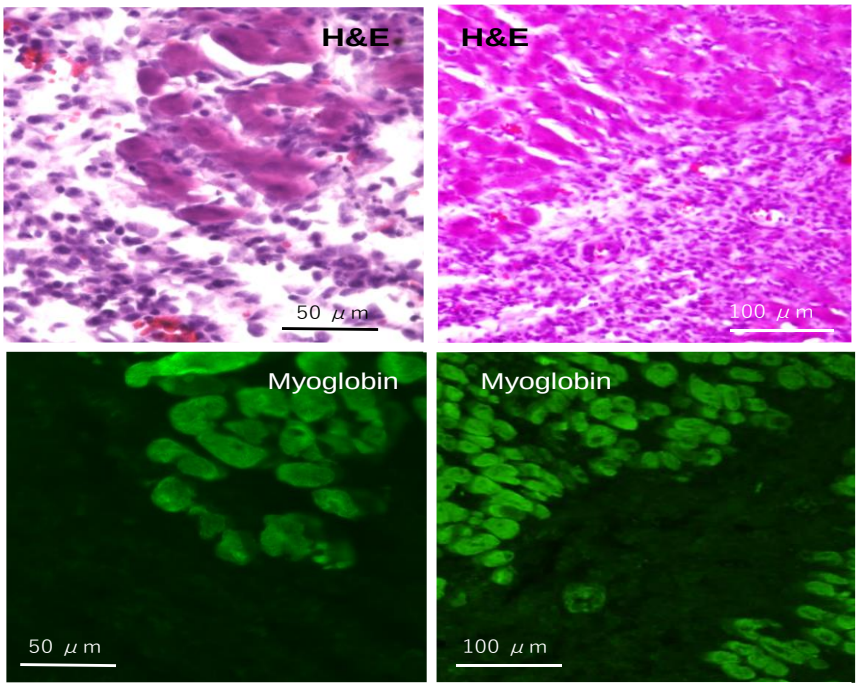

Figure A

The H&E (upper panels) and IHC staining for myoglobin (lower panels) of infarcted myocardium are shown in the same slice (left panels) in a high magnification and in a low magnification (right panels). While H&E staining makes it difficult to identify viable cardiomyocytes, IHC staining clearly demarcates viable myocardium.

Figure B

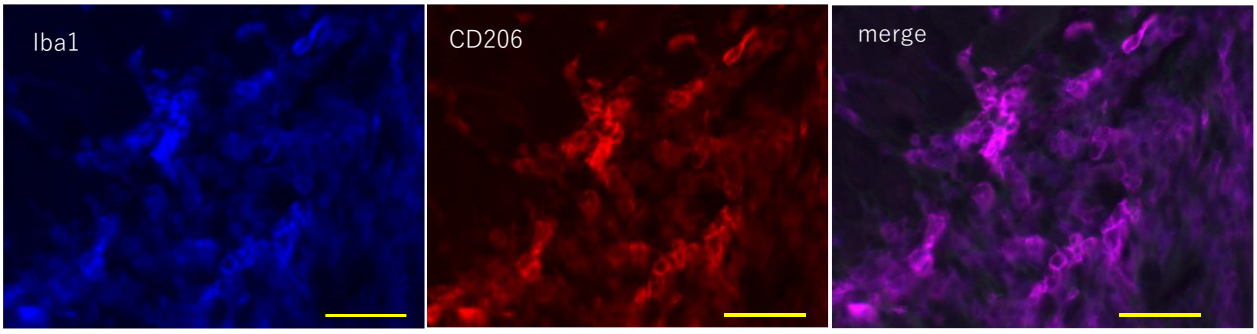

Figure B. Dual IHC staining for Iba1 and CD206

In the infarcted myocardium of a SG rat (4d) stained for Iba1 (left), CD206 (middle), and merge (right) showed that most of the Iba1-positive cells were also positive for CD206, suggesting that infiltrating cells were mostly CD206-positive, type-2 macrophages[78]. Length of bar is 20 μm.

SUPPLEMENTS

Supplement 1. Abbreviations in Alphabetical Order

BAX	Bcl-2-associated X protein
BNP	Brain-type Natriuretic Peptide
C3aR1	Complement C3a receptor 1 (C3ar1), mRNA
Casp 3	Caspase 3
CCL2	C-C motif chemokine ligand 2 (Ccl2), mRNA
Clec3a	C-type lectin domain family 3, member A (Clec3a), mRNA
COHb	Fraction of carboxy-Hb (%)
EDP	End-diastolic pressure (mmHg)
EDPVR	End-diastolic pressure-volume relationship
ESP	End-systolic pressure (mmHg)
ESPVR	End-systolic pressure-volume relationship
FS	LV Fractional Shortning (%)
H&E	hematoxylin and eosin
HBOCs	Hemoglobin-based Oxygen Carriers
HIF-1α	hypoxia inducible factor 1-α
HO-1	Heme Oxygenase 1
HO-2	Heme oxygenase 2 (Hmox2), transcript variant 1, mRNA
Hsp90AA1	Heat shock protein 90, alpha (cytosolic), class A member 1, mRNA
Iba1	Ionized calcium-binding adapter molecule 1
IHC	Immunohistochemical
LVDD	LV end-diastolic dimension (mm)
LVSD	LV end-systolic dimension (mm)
Max+dP/dt	Max positive dP/dt (mmHg/mL)
Max-dP/dt	Max negative dP/dt (mmHg/mL)
MetHb	Fraction of Met-Hb (%)
MI	Myocardial infarction
NFKb1	Nuclear factor kappa B subunit 1, mRNA
NOS3	Nitric oxide synthase 3, mRNA
Nqo-1	NAD(P)H Quinone Dehydrogenase-1
Nrf2	Transcription factor NF-E2-related factor 2
O_2Hb	Fraction of Oxygen-Hb (%)
$P_{50}O_2$	The partial pressure of O_2 where half of hemoglobin is oxygenated
PCR	Polymerase-chain reaction
PDGFRβ	Platelet-derived growth factor receptor β
PEG	Polyethylene glycol
PVR	Pressure-volume relationship
RBC	Red blood cells
SG	Sanguinate® PEGylated Carboxyhemoglobin Bovine
SV	Stroke volume (μL)
tHb	Total Hb (g/dL)
TNFα	Tumor necrosis factor α
VEGF	Vascular endothelial growth factor

Supplement 2. List of PCR primers used in the current study

	Sense Primer	Antisense Primer
β-actin	AGCCATGTACGTAGCCATCC	CTCTCAGCTGTGGTGGTGAA
Bax	AGGATCGAGCAGAGAGGATG	AAACATGTCAGCTGCCACAC
BNP	CTGGGAAGTCCTAGCCAGTCT	GTCTATCTTCTGCCCAAAGCAG
C3ar1	ATCAGTCCTGGAGCCTTCTG	AGGCCGTGAGTGTAGGTCAG
Caspase 3	GAAACCTCCGTGGATTCAAA	TAGCTGCATCGACATCGGTA
CCL2	AGCATCCACGTGCTGTCTC	GATCATCTTGCCAGTGAATGAG
Clec3a	ATGCCTTGAAGGAAATGCAA	TATGAACTTTGGTGCCTCGAA
Cxcr3	AAGCAGGCAGCACGAGAC	GGCATCTAGCACTTGACGTTC
HIF-1α	TGCTCATCAGTTGCCACTTC	CCATCCAGGGCTTTCAGATA
Hmox-2	TGAAAGGAAACATTAAGAAGGAGCTA	TCCTCAAGGGCTGAGTATGTG
Hmox-1	AGCATGTCCCAGGATTTGTC	ACTGGGTTCTGCTTGTTTCG
Hsp90AA1	TTCTGCCAAGATGCCTGAG	AAGGCAAAGGTTTCGACCTC
IL-10	AGTGGAGCAGGTGAAGAATGA	CACGTAGGCTTCTATGCAGTTG
IL-1b	TGTGATGAAAGACGGCACAC	CTTCTTCTTTGGGTATTGTTTGG
IL-6	AGAGCAATACTGAAACCCTAGTTCA	AGGAGAGCATTGGAAGTTGG
NFKb1	TCATCAACATGAGAAACGATCTG	CTCAGCAAGTCCTCCACCA
NOS2	GCCCAGAGTCTCTAGACCTCAA	CATGGTGAACACGTTCTTGG
NOS3	TGACCCTCACCGATACAACA	CGGGTGTCTAGATCCATGC
Nqo-1	CGCAGAGAGGACATCATTCA	CGCCAGAGATGACTCAACAG
Nrf2	GCAACTCCAGAAGGAACAGG	GGAATGTCTCTGCCAAAAGC
TNF	CGTAGCCCACGTCGTAGC	GGTTGTCTTTGAGATCCATGC

Supplement 3. List of antibodies and chemicals used in the current study

Peptide / Protein Target	First antibody	Catalog No Manufacturer Providing the Antibody	Species Raised in; Monoclonal or Polyclonal	Dilution Used
Myoglobin	Anti-myoglobin	b77232, Abcam	rabbit, monoclonal	1:150
Iba1	Anti-Iba1	019-19741, Wako	rabbit, polyclonal	1:500
CD206	Anti-CD206	AF2535, D&D Systems	goat, polyclonal	1:250
PDGFRβ	Anti-PDGFRβ	ab32570, Abcam	rabbit, monoclonal	1:200
TNF-α	Anti-TNFα	11948, Cell Signaling	rabbit, monoclonal	1:200
HO-1	Anti-HO1	SMC-131, Stress Marq	mouse, monoclonal	1:200
HIF-1α	Anti-HIF1α	sc-13515, Santa Cruz	mouse, monoclonal	1:200
VEGF	Anti-VEGF	sc-7269, Santa Cruz	mouse, monoclonal	1:200
SG	Anti-SG	Prolong Pharmaceuticals	rabbit, polyclonal	1:250

	Second antibody		Catalog Number Manufacturer	Dilution Used
	Alexa fluor 594	donkey anti gooat	A-11058, Molecular Probe	1:500
	Alexa fluor 594	donkey anti mouse	ab150108, Abcam	1:500
	Alexa fluor 488	donkey anti mouse	ab150105, Abcam	1:500
	Alexa fluor 488	donkey anti rabbit	A21206, Invitrogen	1:500
	Alexa fluor 594	donkey anti rabbit	A21207, Invitrogen	1:500
	Alexa fluor 647	donkey anti rabbit	A-31573, Thermo Fisher	1:500